Numerical Simulation of the Electrical Double Layer Based on the Poisson-Boltzmann Models for AC Electroosmosis Flows

Pascale Pham*[(1)], Matthieu Howorth[(1)], Anne Planat-Chrétien[(1)] and Sedat Tardu[(2)]

[(1)]CEA/LETI - Département des microTechnologies pour la Biologie et la Santé
[(2)]LEGI, UMR 5519, B.P. 53 X 38041 Grenoble Cedex France
*corresponding author: 17 Avenue des Martyrs, 38054 Grenoble cedex 9, France, pascale.pham@cea.fr

Abstract: In this paper, the analytical validation of Poisson-Boltzmann (PB) equation computed with Comsol Multiphysics™, in the case of a polarized surface in contact with the electrolyte [1]-[2], is first presented. Comsol Multiphysics™ algorithms easily handle the highly nonlinear aspect of the PB equation. The limitations of the PB model, that considers ions as pointlike charges, are outlined. To account for the steric effects of the ion crowding at the charged surface, the Modified Poisson-Boltzmann model, proposed by Kilic et al. [3], is analysed for symmetric electrolytes. The MPB equation is then coupled to the complex AC electrokinetic and the Navier-Stokes equations to simulate the AC electroosmosis flow observed inside an interdigitated electrodes microsystem [4]-[6].

Keywords: numerical simulation, Poisson-Boltzmann, Finite Element Method, AC electrokinetics.

1. Introduction

The Electrical Double Layer (EDL) represents the interface between a solid surface (polarized electrode) and an electrolyte. The charged surface attracts nearby counterions and repels coions present in the solution. In microsystems, the same electrostatic phenomenon is also present around charged nanoparticles (biomolecules, latex beads…) immersed into an electrolyte: they experience electrostatic interactions which give rise to a counterion cloud. The EDL or the counterion cloud is likely to react to the applied electric fields and can strongly influence various electrical phenomena such as dielectrophoresis, electrophoresis of polyelectrolytes (DNA, proteins,…) or AC electrokinetic flows.

RC circuit models are widely used by electrochemists for representing the EDL. However, in microsystems where applied electric fields can be very strong because of the very small dimensions, this approximation fails [3] [7]. Despite the explosive growth of multiscale modeling for microfluidics, where the continuum is usually coupled to Molecular Dynamics techniques, we investigated here the use of coupled continuum models, based on the Poisson-Boltzmann (PB) equation. For us, it is interesting to represent the EDL using the Comsol Multiphysics™ software application because its strong coupling to macroscopic equations (Navier-Stokes in our case) is possible.

2. Theory

2.1 The electrical double layer

In this paper, we consider that electrodes are ideally polarizable i.e. that no electron transfer (electrochemical) reactions occur at the electrode. The model which gave rise to the term 'electrical double layer' was first put forward in the 1850's by Helmholtz. In order for the interface to remain neutral, the charge held on a polarized electrode is balanced by the redistribution of ions close to the electrode surface. In Helmholtz's view of this region, the attracted ions are assumed to approach the electrode surface with a distance assumed to be limited to the size of the ion: the overall result is two layers of charge (the double layer) and a linear potential drop which is confined to this region only. A later model put forward by Gouy and Chapman supposed that ions are able to move in solution and so the electrostatic interactions are in competition with Brownian motion. The result is still a region close to the electrode surface containing an excess of one type of ion but now the potential drop is exponential and occurs over the region called the diffuse layer:

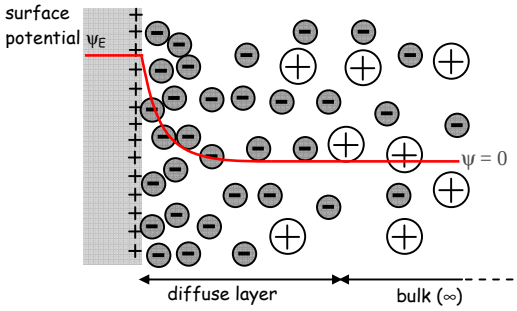

Figure 1. The Gouy-Chapman representation of the EDL used by the PB equation.

The most common representation of the Electrical Double Layer (EDL) is due to Stern (1924): the EDL is composed of two layers (see Figure 2). The inner layer (called the compact layer) which is in contact with the electrode and where ions are absorbed on to the surface due to high electrostatic interactions. Outside the compact layer, there is the diffuse double layer:

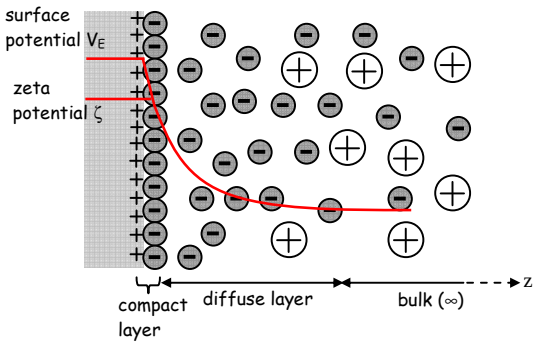

Figure 2. The Stern representation of the EDL composed of the compact layer and the diffuse layer. The variation of the electrical potential V thru the EDL (red line) is represented for the case of a positively charged surface.

The potential at the interface between the compact and the diffuse layer is called the zeta potential ζ which can be determined from electrokinetics measurements.

2.2 The Poisson-Boltzmann equation

The Poisson-Boltzmann (PB) theory is based on the Gouy-Chapman representation [3]. The diffuse layer is considered to be directly in contact with the charged surface who's potential or charge is known (see Figure 1).

We will see in this section that the PB theory predicts that the surface potential decreases exponentially in the EDL. This is the screening phenomenon of the surface charges by the counterions.

Because the PB equation has limitations (see section 3.2), we voluntary name the electric potential used in the PB equation by ψ instead of V used in the Stern representation (Figure 2). In the PB equation, ions are supposed to be pointlike charges, the ionic solution is supposed to be a dilute solution (so the ions do not interact with each other) and the solvent (water) is considered as a continuum dielectric of permittivity $\varepsilon = \varepsilon_0 \varepsilon_r$. The charges of the surface induce an electric potential ψ (V) in the electrolyte which acts on each specie of ions. Each ion concentration distribution c_i (ions/m^3) is given by the Boltzmann distribution where electrostatic ($z_i e\psi$) and thermal (kT) energies balance each other:

$$c_i = c_i^{\infty} \, e^{-\frac{z_i e \psi}{kT}} \qquad (1)$$

$c_i^{\infty} = n_i c^{\infty}$ is the ion i concentration in the bulk (n_i being the number of ions i in the electrolyte formula, c^{∞} is the bulk concentration), T is the temperature (K) and k the Boltzmann constant (1.38 10^{-23} J/K). e is the proton charge (1.6 10^{-19}C) and z_i is the ion i charge number. For convenience, concentrations can be expressed in Molar unit (M = mole/L): $M_i = 10^3 c_i \, N_A$ where N_A is the Avogadro's number (6.022 10^{23}).

Each ion distribution corresponds to a volume free charge distribution q_i such that:

$$q_i = z_i e \, c_i \qquad (2)$$

In return, the total free charge density

$$q = \sum_i q_i = \sum_i z_i e \, c_i \qquad (3)$$

acts on the potential distribution thru the Poisson equation which links the electric potential ψ to its sources (q):

$$\vec{\nabla}.\left(-\varepsilon \vec{\nabla}\psi\right) = q \qquad (4)$$

Combining (4) with (1) gives rise to the non linear Poisson-Bolztmann (PB) equation:

$$\vec{\nabla}.\left(-\varepsilon\vec{\nabla}\psi\right)=\sum_i z_i e c_i^{\infty}\, e^{-\frac{z_i e\psi}{kT}} \quad (5)$$

The boundary conditions associated to the PB equation are the classical ones used in electrostatics (see Figure 3). On the electrode E, the potential ψ_E corresponds to the following surface charge density [8]:

$$\sigma_E = \vec{D}.\vec{n} = -\varepsilon\left.\frac{\partial\psi}{\partial n}\right|_E \quad (6)$$

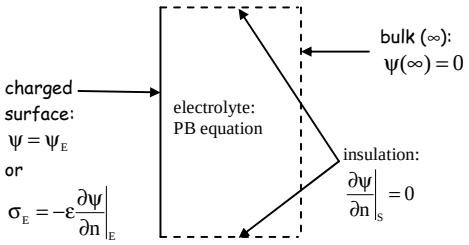

Figure 3. Boundary conditions associated to the PB equation for a 2D semi-infinite electrolyte in contact with a flat charged surface.

In the particular case of a binary symmetric electrolyte (for example KCl or $MgSO_4$, $z_+ = |z_-| = z$, $c_+^{\infty} = c_-^{\infty} = c^{\infty}$), the PB equation becomes the Gouy-Chapman (GC) equation [1] [3]:

$$\vec{\nabla}.\left(-\varepsilon\vec{\nabla}\psi\right) = -2\,z\,e\,c^{\infty}\sinh\left(\frac{z\,e\psi}{kT}\right) \quad (7)$$

2.3 The Debye-Huckel theory: the linearized PB equation

The linearization of the GC equation is obtained under the assumption that the electrostatic energy is small compared to the thermal energy:

$$|\psi| << \psi_T = \frac{kT}{z\,e} \quad (8)$$

At room temperature (298 K), for monovalent ions (z = 1) ψ_T ~ 26 mV, for divalent ions, ψ_T ~ 13 mV. Under assumption (8), equation (10) can be linearized:

$$\vec{\nabla}.\left(-\varepsilon\vec{\nabla}\psi\right) = -\frac{2z^2e^2c^{\infty}}{kT}\psi \quad (9)$$

This equation admits the following solution:

$$\psi(z) = \zeta e^{-\frac{z}{\kappa^{-1}}} \quad (10)$$

When moving away from the polarized electrode, the potential decreases exponentially with a characteristic length κ^{-1} called the Debye length:

$$\kappa^{-1} = \sqrt{\frac{\varepsilon\,kT}{2z^2e^2c^{\infty}}} \quad (11)$$

The Debye length (λ_D) is widely used to estimate the EDL thickness because its simple formula depends only on the electrolyte characteristics. In this paper, we always consider the case of an aqueous electrolyte (ε_r = 78.5) at ambient temperature (298 K).

3. Numerical simulation of the PB and the MPB equations

Using the Debye-Hückel theory is quite restrictive for microsystems because applied electrode potentials are often much greater than ψ_T. The PB equation is highly non linear and our first concern is evaluating how Comsol Multiphysics™ and the Finite Element Method can handle this difficulty.

3.1 Analytical validation of the PB equation

The PB equation is implemented in Comsol Multiphysics™ as a PDE equation. The validation of the PB numerical model is made by the comparison of numerical solutions from PB and GC equations (5) and (7) with analytical solutions in the case of binary symmetric semi-infinite electrolytes in contact with a flat polarized surface [1]:

$$\psi(z) = \frac{4kT}{ze}\arctan h\left[\tanh\left(\frac{ze\psi_E}{4kT}\right)e^{-\kappa z}\right] \quad (12)$$

Tests are performed on the geometry of Figure 3 for two different types of electrolytes (1:1 and 2:2), variable bulk concentrations, variable surface potentials ψ_E. In the two following figures, the curves were drawn for surface potentials ψ_E of +50 mV and +1V and bulk concentrations c^{∞} of 0.01M and 0.1M.

The numerical solution of both the CG equation (5) and the PB equation (7) is in a good agreement with the analytic solution (12).

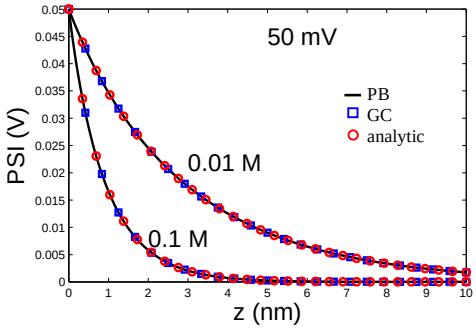

Figure 4. Comparison of numerical (black = PB, blue = GC) and analytical (red) electric potentials for a 1:1 electrolyte at bulk concentrations of 0.01 M and 0.1 M. ψ_E = +50mV. z (nm) is the distance from the electrode surface.

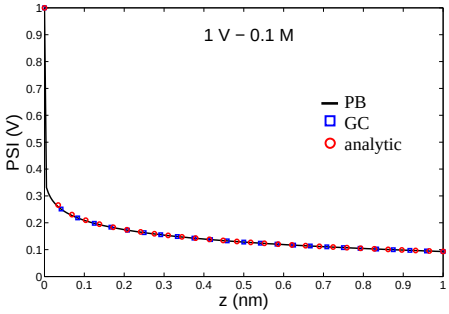

Figure 5. Comparison of numerical (black = PB, blue = GC) and analytical (red) electric potentials for a 1:1 electrolyte at bulk concentration of 0.01 M and ψ_E = +1V.

Figure 6 compares the Debye length with the EDL width (L_{EDL}) computed from the PB and the GC solutions according to the bulk concentration of a KCl electrolyte, for the applied voltage +0.1V. As expected, the Debye length underestimates the EDL width and the error committed when using (11) is quite important. It increases with the bulk concentration.

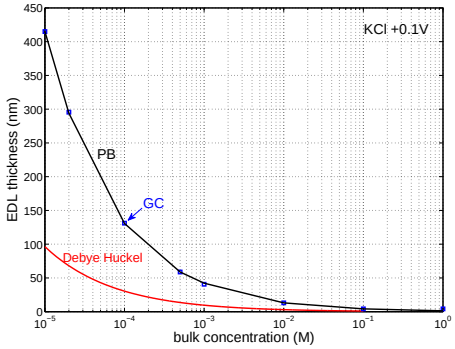

Figure 6. The EDL width L_{EDL} according to the bulk concentration for KCl, at +0.1V: from GC solution (blue), PB solution (black) and Debye length formula (11) (red).

3.2 Limitations of the PB equation validity

One could expect that the PB equation (and the GC equation for binary symmetric electrolytes), when fully solved in the non linear regime ($\psi > \psi_T$), would give a good estimation of the EDL. However, even at large applied potentials, the PB and the CG equations have limited applicability.

One of the assumptions made in the PB equation is that ions are pointlike charges. This means that the ions are considered to have no size. The consequence is that the PB equation can predict an infinite concentration of counter-ions near the charged surface, which is not realistic. For example, for the aqueous electrolyte (Na^+, Cl^-), at a bulk concentration of 1 mM, ambient temperature and ψ_E = +1V, the surface charge calculated from expression (6) corresponds to a concentration of spherical counter-ions (Cl^-) of 5 10^{40} ions/m^3 hence 8.3 10^{16} M! This would mean that the chloride ion radius is 1.5 10^{-14}m which is 10 000 times smaller than the real value. Here we use the numerical PB model to determine the area in which the PB equation is valid, the limit being given by the steric effect which corresponds to a maximum concentration reached at the charged surface due to the hydrated ion crowding.

	Na^+	K^+	Mg^{2+}	Cl^-	SO_4^{2-}
hydrodynamic radius (nm) [9]	0.184	0.125	0.444	0.121	0.230
maximum concentration (ions/m^3) for a face centred cubic packing [10]	$2.85\ 10^{28}$	$9.01\ 10^{28}$	$2.72\ 10^{27}$	$1.008\ 10^{29}$	$1.45\ 10^{28}$
maximum concentration (M)) for a face centred cubic packing	47.3	150	4.53	167	24
maximum concentration (M) for Kilic MPB model [3]	33.33	106.31	1.42	117.2	17.07

Table 1. Examples of hydrodynamic radius and maximum concentration representing the steric limit for several ions.

In Table 1, the steric limit is estimated from the face centred cubic sphere packing model [10] for which the packing density is 0.74 and from the Kilic model [3] where each ion of diameter a is supposed to occupy a volume equals to a^3.
Using the steric limit values of Table 1 (for the face centred cubic model), Figure 7 reports the PB equation validity domains in terms of the applied voltage ψ_E and the bulk concentration fora KCl and $MgCl_2$. These calculations show that the PB validity domain beyond the linear approximation is restricted to voltages of several hundreds of mV.

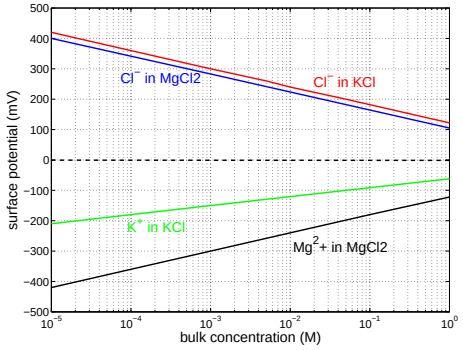

Figure 7. Validity domains of the PB equation for KCl and $MgCl_2$ electrolytes.

3.3 The Modified Poisson-Boltzmann (MPB) equation

Recently, an equation taking into account the steric effects of the ions has been proposed by Kilic et al [3]. It is called the Modified Poisson-Boltzmann (MPB) equation.

In the MPB equation, the Boltzmann distribution part of the PB equation is modified. The modified Boltzmann distribution is given by the following expression:

$$c_i = \frac{c_i^{\infty}\, e^{-\frac{z_i e \psi}{kT}}}{1 + 2\nu \sinh^2\left[\frac{z_i e \psi}{2kT}\right]} \qquad (13)$$

where ν is the packing parameter such as $\nu = 2a^3 c^{\infty}$ and a is the effective ion size. We consider here a as the diameter of the hydrated ion, see Table 1.
For a binary symmetric z:z electrolyte, the MPB equation can be written as follows [3]:

$$\vec{\nabla}.\left(-\varepsilon\vec{\nabla}\psi\right) = -z e c^{\infty} \frac{2\sinh\left[\frac{z_i e \psi}{2kT}\right]}{1 + 2\nu \sinh^2\left[\frac{z_i e \psi}{2kT}\right]} \qquad (14)$$

The MPB equation (14) can be generalized to non symmetric electrolytes by combining (13) with (4).
In Figure 8, formula (13) is plotted versus the applied voltage ψ_E and compared to the PB distribution (1). The PB distribution predicts a continuous increase of the concentration of the ions at the surface with the surface potential. With the MPB distribution, the concentration of each ion saturates and cannot exceed the steric limit given by a^{-3}.

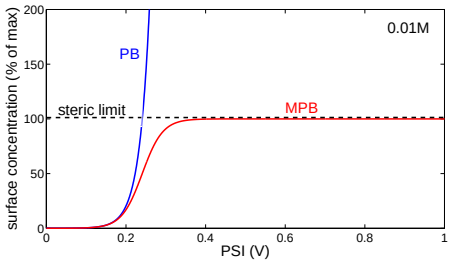

Figure 8. Comparison of the surface concentration (% of the maximum concentration given by the steric limit) for the PB distribution (blue) and the MPB distribution (red) according to the positive applied voltage. The anion is Cl^- and its bulk concentration is 0.01M.

On Figure 9, the MPB equation has been solved for quasi-linear conditions (+0.1V, 0.01M for KCl): as expected, the MPB solution and the PB solution are identical.

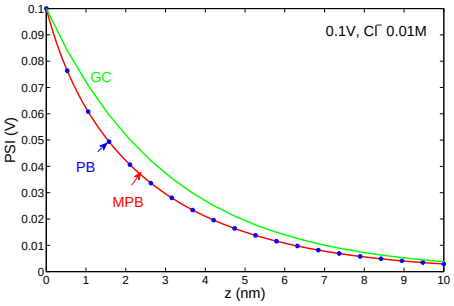

Figure 9. Validation of the MPB equation on a quasi-linear case (KCl electrolyte, +0.1V, 0.01 M) by comparison with PB and GC solutions.

For higher voltages (+1V, see Figure 10), the MPB and PB solutions do not overlap anymore because the PB equation validity fails. The MPB equation predicts an EDL width much bigger (~ 0.2 nm) than the one given by the PB solution (<< 0.01 nm). The crowding effect at the charged surface repels the counterions into the diffuse layer and provides a much larger EDL width than what the PB equation is predicting.

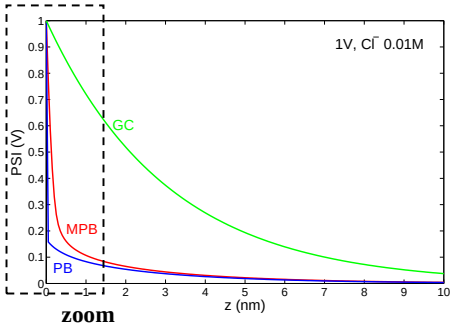

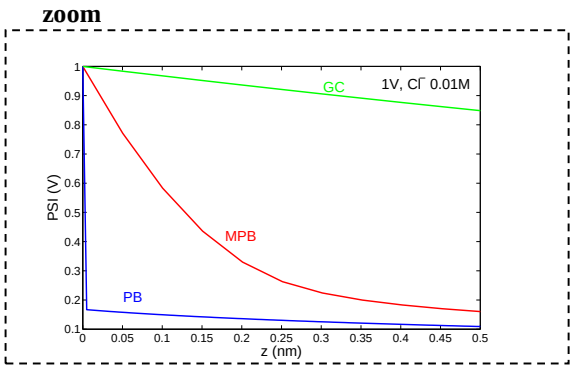

Figure 10. PB, MPB and GC solutions for a KCl electrolyte of bulk concentration 0.01M and a high surface potential (+1V). The lower figure is a zoom of the upper one near the charged surface.

Next figure plots the chloride concentration profile corresponding to the previous potential profile: near the charged surface, the curve clearly shows that the MPB model limits the concentration to its maximum value (117 M for Cl^-, see Table 1):

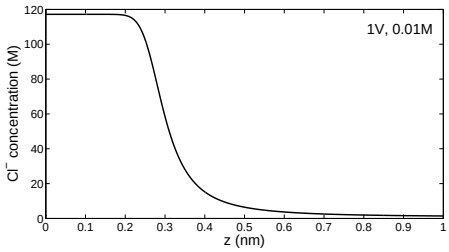

Figure 11. The Cl^- concentration profile given by the MPB equation for a KCl electrolyte of bulk concentration 0.01M and a high applied surface potential (+1V).

3.4 Getting convergence during the PB and the MPB equation computation

The previous numerical results show that the higher the electrode potential ψ_E is, the higher the non linearity of the problem is. To obtain a good convergence of the solution, several 'tricks' are used. First, the mesh is highly refined near the electrode surface where gradients are very steep. The one dimensional character of the solution allows the use of quadrilateral elements with low quality: the 'mapped' mesh has the advantage to reduce drastically the total number of Finite Elements and so the solution time and the memory requirements. Second, previous solutions obtained from the GC solution and/or

with lower applied voltages were used as initial condition by selecting the 'restart button'.

4. Coupling the MPB equation with the Navier-Stokes equation for AC electroosmosis

AC electroosmosis is the fluid flow induced above a charged surface by the drift of the EDL mobile charges by the electric field. The convection of the free charges in the EDL can be neglected in comparison with their drift [11] leading to a weak coupling between the electrical stress and the fluid flow.

In most papers which deal with ac electroosmosis modeling, the thin double layer approximation under the linear regime is used for the EDL [4]-[6]. The EDL is estimated from the Debye-Hückel theory and is not included inside the computation domain. The electric field inside the bulk is computed with the ac electrokinetic equation (see (16)) connected to the EDL thru a Neumman boundary condition (18). The fluid motion is obtained from the Navier-Stokes equation (20) where the electrical stress acts as a slip velocity imposed as a boundary condition on the electrode surface. This slip velocity is estimated from empirical parameters (the capacitance of the compact and the diffuse layers) and the tangential component of the electric field given by (16).

Our goal here is to take off these empirical parameters from the numerical model. This supposes that the EDL is fully represented inside the computation domain for the fluid motion. The electrical volume force acting inside the EDL on the fluid is not transformed into a slip velocity. The numerical difficulty here is the multiscale coupling that has to be performed: the EDL, which is tens of nm wide, has to be included in a microsystem which size reaches 1 mm.

4.1 Ac electroomosis equations

In our numerical model, we use the MPB equation to estimate more precisely the EDL features: the EDL width for the electric field calculation inside the bulk and the free charge density for the velocity field.

The EDL is assumed to be a capacitance per unit area C_{EDL} (C/m^2) such that:

$$C_{EDL} = \frac{\varepsilon}{L_{EDL}} \tag{15}$$

where L_{EDL} is the EDL width computed from the MPB equation (14).

Under AC voltages of angular frequency ω, the electric field inside the bulk (i.e. outside the EDL) is given by the ac complex electrokinetic equation for real dielectrics [11]-[12]:

$$\vec{\nabla}.\left(-(\sigma + i\omega\varepsilon)\vec{\nabla}V^*\right) = \vec{\nabla}.\left(-\sigma^*\vec{\nabla}V^*\right) \tag{16}$$

where σ is the bulk conductivity (S/m) , V* the complex electrical potential of real part Re(V*) = V and σ* the complex conductivity.

On insulated surfaces in contact with the electrolyte, the boundary condition associated to (16) is of Neumann homogeneous type:

$$\mathrm{Re}\left(-\sigma^*\frac{\partial V^*}{\partial n}\right) = 0 \tag{17}$$

with n being the outer normal.

Above the charged electrodes, which are assumed perfectly polarizable (no electrochemical reactions), the bulk is in contact with the EDL. Equation (16) is connected to the MPB equation at this interface where the conservation of the normal current density gives:

$$\mathrm{Re}\left(-\sigma^*\frac{\partial V^*}{\partial n}\right) = i\omega\, C_{EDL}\, \Delta\psi_{EDL} \tag{18}$$

where $\Delta\psi_{EDL}$ is the potential drop across the EDL:

$$\Delta\psi_{EDL} = \psi_E - V \tag{19}$$

and C_{EDL} is given by (15).

The time-averaged fluid flow is obtained from the Navier-Stokes equation where effects from the Joule heating are supposed to be negligible:

$$\vec{\nabla}p - \eta\nabla^2\vec{v} + \rho_m\left(\vec{v}.\vec{\nabla}\right)\vec{v} = \left\langle\vec{F}_E\right\rangle \tag{20}$$

ρ_m is the mass density of the fluid (1000 kg/m^3 for water) and η is its dynamic viscosity (10^{-3} kg/m/s for water). Because Reynolds numbers are very low in microsystems [12], the inertia term is generally very low in (20).

$\left\langle \vec{F}_E \right\rangle$ is the time-averaged electrical force due to the interaction of the ac electric field with the free charges of the EDL. Under the assumption that the fluid permittivity is uniform (which is not generally the case for high voltages [7]):

$$\left\langle \vec{F}_E \right\rangle = \frac{1}{2} q \, \mathrm{Re}(\vec{E}^*) \qquad (21)$$

where q is the free charge density inside the EDL defined by (3) and computed from the source term of the MPB equation (14). As the MPB equation involves only the diffuse layer of the EDL, the boundary above the electrodes for equation (20) represents the interface between the compact layer and the diffuse layer: the boundary condition of type 'slip/symmetry', which is equivalent to the nonpermeability condition, is used at this interface (see figure 12):

$$\vec{v}.\vec{n} = 0 \qquad (22)$$

This condition is also used on other boundaries because the vertical ones are symmetry planes and the upper one is supposed to be a free surface.

4.2 Numerical settings

The 2D interdigitated electrode microsystem studied by Green and al. [4] is considered here: the electrode width is 500 µm for a gap of 25 µm. The electrolyte thickness above the electrode plane is about 1 mm. The electrolyte is a KCl solution of conductivity 2.1 mS/m (electrolyte A): as the authors don't specify the corresponding bulk concentration, we use the Kohlraush's law to estimate it [9]: $1.4\ 10^{-4}$ M.

The diagram of Figure 12 summarizes the way couplings between equations are done in our AC electroosmosis model: the MPB equation (blue) is solved on a 1D geometry, the EDL width L_{EDL} is computed from the 1D potential by using an integration coupling variable: it is used in formula (18) for the boundary condition above electrodes of the AC complex electrokinetic equation (green).

The free charge density (source term of (14)) is extruded from the 1D geometry into the 2D geometry for the solving of the Navier-Stokes equation (red).

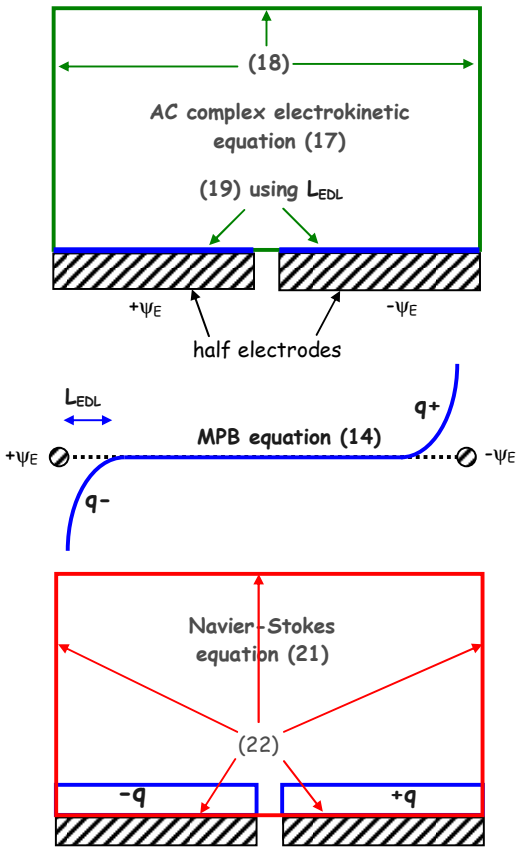

Figure 12. Equations coupling for the AC electroosmosis model. The electrodes shown as black hashed areas do not take part of the domain computation.

4.3 Numerical results

The following figures give examples of numerical results obtained with the AC electroosmosis model described in this paper, for the case $\psi_E = \pm 0.1$V.

On Figure 13, the electric field and the potential is represented according to the frequency. By looking at the maximum value of the potential, we can see that, for 100 Hz, not all the maximum potential inside the bulk is only 0.04V compared to the electrode value which is 0.1V: a big part of the electrical potential drop occurs inside the EDL. On the contrary, the EDL does not influence anymore the potential distribution inside the bulk when frequency reaches 1 kHz.

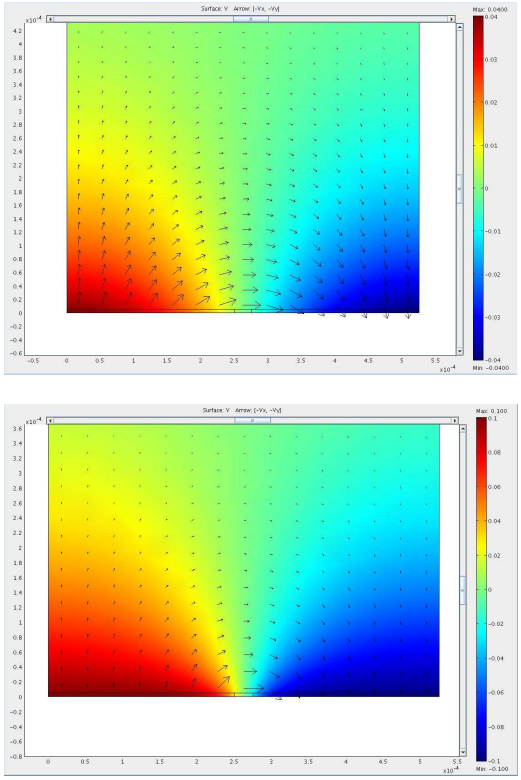

Figure 13. Isopotentials (V) and electric field vectors inside the bulk for $\psi_E = \pm 0.1$V, 100 Hz (upper) and 1 kHz (lower).

The next Figure shows the corresponding velocity field (white) and its magnitude (isovalues) for the 2 frequencies. Maximum velocity is reached at the electrode surface (red areas), near the gap. The fluid flow distribution is varying with frequency but seems in good agreement with the Green's observations [4].

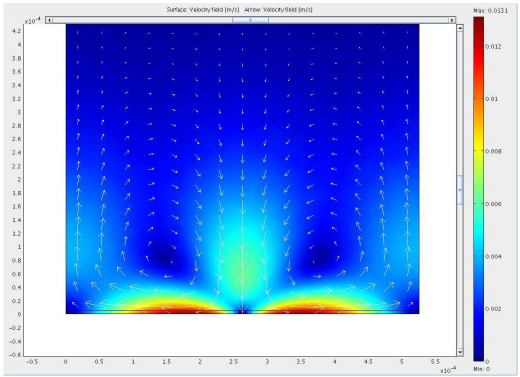

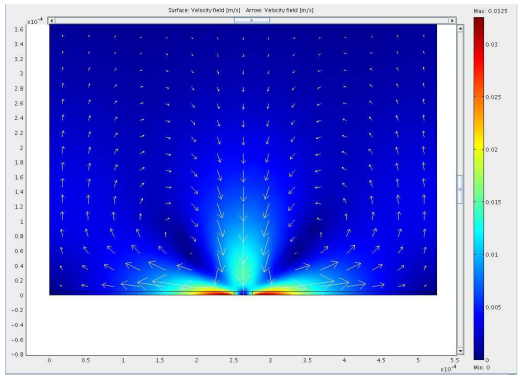

Figure 14. Velocity magnitude (m/s) and velocity vectors inside the bulk for $\psi_E = \pm 0.1$V, 100 Hz (upper) and 1 kHz (lower).

The maximum velocity values obtained for these two configurations (0.013 m/s at 100 Hz and 0.032 m/s at 1 kHz) seem to be very high when comparing them to Green's measurements [4] (about hundreds of μm/s). This is maybe due to the boundary condition type we selected for the computation of the fluid motion (slip condition). Obviously, a no slip condition should diminish the maximum velocity (0.0027 m/s at 1 kHz), as shown by the following figure:

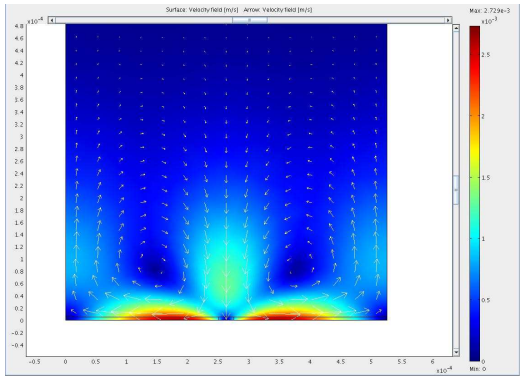

Figure 15. Velocity field when using a no slip boundary condition at the interface between the diffuse layer and the compact layer (1 kHz).

5. Conclusions

In this paper, we propose a numerical model implemented into Comsol Multiphysics™ for the modeling of the ac electroomosis phenomena. In this model, no empirical parameters are necessary to compute the velocity field.
The analytical validation of PB equation and its comparison with the MPB equation proposed by Kilic et al. [3] at low voltages show that Comsol Multiphysics™ algorithms easily handle the highly nonlinear aspect of these equations. The weak coupling between the 1D MPB equation with the 2D complex AC electrokinetic and the Navier-Stokes equations has been computed on the interdigitated electrodes microsystem studied by Green [4]. The first numerical results seem to be in a good agreement with Green's results. Navier-Stokes convergence could be improved by using a nonprimitive set of variables (stream function and vorticity) instead of the velocity and the pressure [13]. A more detailed analysis of the Green's interdigitated electrodes microsystem must be continued to fully validate the model.

.

6. References

[1] L. Renaud, 'Etudes de systèmes microfluidiques : application à l'électrophorèse sur puces polymères', Thèse de Doctorat, Université Claude Bernard – Lyon1, juillet 2004.
[2] M.Z. Bazant, K. Thornton, A. Adjari, 'Diffuse-charge dynamics in electrochemical systems', *Physical review E* 70, 021506 (2004).
[3] M.S. Kilic, M.Z. Bazant, 'Steric effects in the dynamics of electrolytes at large applied voltages. I. Double-layer charging', *Physical Review E* **75**, 021502 (2007).
[4] N. G. Green, A. Ramos, A. Gonzales, H. Morgan , A. Castellanos,'Fluid flow induced by nonuniform ac fields in electrolytes on microelectrodes. III Observation of streamlines and numerical simulation', *Physical review E*, **66** 026305 (2002).
[5], A. Ramos, H. Morgan , N G Green, A. Castellanos, 'AC Electrokinetics: a review of forces in microstructures', *J. Phys. D: Appl. Phys.* **31** (1998) 2338-2353.
[6] S. Tardu, 'The electrical double layer effect on the microchannel flow stability and heat transfer', *Superlattices and Microstructures* **35** (2004) 513-529.
[7] M.Z. Bazant, K. Thornton, A. Adjari, 'Diffuse-charge dynamics in electrochemical systems', *Physical review E*, **70** 021506 (2004).
[8] E. Boridy, 'Electromagnétisme, théories et applications', ISBN 2-7605-0376-3, 1990.
[9] P.W. Atkins, 'Physical Chemistry', 5th edition, ISBN 0-19-855731-0, 1994.
[10] Conway, J. H. and Sloane, N. J. A. Sphere Packings, Lattices, and Groups, 2nd ed. New York: Springer-Verlag, 1993.
[11] P. Pham, A.S. Larrea, R. Blanc, F. Revol-Cavalier, I. Texier, F. Perraut, 'Numerical design of a 3D microsystem for DNA dielectrophoresis: the pyramidal microdevice', *Journal of Electrostatics*, 65 (2007) 511-520.
[12] A. Castellanos, A. Ramos, A. Gonzales, N G Green, H. Morgan, 'Electrohydrodynamics and dielectrophoresis in Microsystems: scaling laws', *J. Phys. D: Appl. Phys.* **36** (2003) 2584-2597.
[13] P. Pham, J.L. Achard, P. Massé, J. Berthier 'Modélisation d'un écoulement Marangoni dans une goutte en équilibre avec sa vapeur', *Journal La Houille Blanche*, vol 5, n°8, 2003.